HHS Public Access

Author manuscript

Ann Surg. Author manuscript; available in PMC 2017 July 01.

Published in final edited form as:

Ann Surg. 2016 July ; 264(1): 169–179. doi:10.1097/SLA.0000000000001364.

THE HUMAN PANCREAS AS A SOURCE OF PRO-TOLEROGENIC EXTRACELLULAR MATRIX SCAFFOLD FOR A NEW GENERATION BIO-ARTIFICIAL ENDOCRINE PANCREAS

Andrea Peloso, MD, PhD[1,#], **Luca Urbani, PhD**[2], **Paolo Cravedi, MD, PhD**[3], **Ravi Katari, BS**[1], **Panagiotis Maghsoudlou, BS**[2], **Mario Enrique Alvarez Fallas, BS**[2,4], **Valeria Sordi, PhD**[5], **Antonio Citro, PhD**[5], **Carolina Purroy, MD, PhD**[3], **Guoguang Niu, PhD**[1], **John P McQuilling, PhD**[1], **Sivanandane Sittadjody, PhD**[1], **Alan C Farney, MD, PhD**[1], **Samy S Iskandar, MBBCh, PhD**[1], **Jeffrey Rogers, MD**[1], **Robert J Stratta, MD**[1], **Emmanuel C Opara, PhD**[1], **Lorenzo Piemonti, MD, PhD**[5], **Cristina Furdui, PhD**[1], **Shay Soker, PhD**[1,^], **Paolo De Coppi, MD, PhD**[2,^], and **Giuseppe Orlando, MD, PhD**[1]

[1]Wake Forest School of Medicine, Winston Salem, NC, USA

[2]Surgery Unit, Stem Cells and Regenerative Section, UCL Institute of Child Health and Great Ormond Street Hospital, London, UK

[3]Department of Medicine, Recanati Miller Transplant Institute and Immunology Institute, Icahn School of Medicine at Mount Sinai, New York, USA

[4]Stem Cells and Regenerative Medicine Lab, Fondazione Instituto di Ricerca Pediatrica Città della Speranza, Padova, Italy

[5]Diabetes Research Institute, IRCCS San Raffaele Scientific Institute, Milan, Italy

Abstract

OBJECTIVE—Our study aims at producing acellular extracellular matrix scaffolds from the human pancreas (hpaECMs), as a first critical step towards the production of a new generation, fully human-derived bio-artificial endocrine pancreas (BAEP). In this BAEP, the hardware will be represented by hpaECMs, while the software will consist in the cellular compartment generated from patient's own cells.

SUMMARY BACKGROUND DATA—ECM-based scaffolds obtained through the decellularization of native organs have become the favored platform in the field of complex organ bioengineering. However, the paradigm is now switching from the porcine to the human model.

METHODS—To achieve our goal, human pancreata were decellularized with Triton-based solution and thoroughly characterized. Primary endpoints were: complete cell and DNA clearance,

Corresponding author: Giuseppe Orlando, MD, PhD, Marie Curie Fellow. Department of Surgery, Section of Transplantation, Wake Forest School of Medicine, Winston Salem, NC, USA. gorlando@wakehealth.edu. Wake Forest Baptist Hospital. Medical Center Blvd, Winston Salem, NC 27157. USA. Tel: +1 336 716 6903. Fax: +1 336 713 5055.

[#]Affiliated to General Surgery, Fondazione IRCCS Policlinico San Matteo and University of Pavia, Pavia, Italy

[*]On behalf of the Carolina Donor Service; °On behalf of LifeShare of The Carolinas

[^]Shay Soker and Paolo De Coppi share the second to last authorship

DISCLOSURE: No conflict of interest to declare by any of the coauthors.

preservation of ECM components, growth factors (GFs) and stiffness, ability to induce angiogenesis, conservation of the framework of the innate vasculature, and immunogenicity. Secondary endpoint was hpaECMs' ability to sustain growth and function of human islet and human primary pancreatic endothelial cells (hPPEC).

RESULTS—Results show that hpaECMs can be successfully and consistently produced from human pancreata, maintain their innate molecular and spatial framework and stiffness, as well as vital GFs. Importantly, hpaECMs inhibit human naïve $CD4^+$ T cell expansion in response to polyclonal stimuli by inducing their apoptosis and promoting their conversion into regulatory T cells. hpaECMs are cytocompatible and supportive of representative pancreatic cell types.

DISCUSSION—We therefore conclude that hpaECMs has the potential to become an ideal platform for investigations aiming at the manufacturing of a regenerative medicine-inspired BAEP.

Mini Abstract

We propose acellular extracellular matrix scaffolds produced from the human pancreas (hpaECMs), as a platform for a new generation, fully human-derived bio-artificial endocrine pancreas (BAEP). hpaECMs maintain the molecular and spatial template of the intact pancreas, are cytocompatible and are able to modulate the immune response.

Keywords

discarded pancreas; diabetes; beta cell replacement; bioartificial pancreas; organ bioengineering and regeneration; scaffold; ECM; decellularization; growth factors; angiogenesis

1. Introduction

Diabetes mellitus [DM] has reached pandemic levels and represents a growing burden both on health-care expenditures as well as the quality and quantity of life for afflicted individuals.[1–4] Exogenous insulin-based intensive glucose control can prevent acute metabolic decompensation and is life-saving in type 1 DM [T1DM], but does not completely protect against the long-term. β-cell replacement through either islet or pancreas transplantation (PTX) are the only therapies able to reliably re-establish a stable euglycemic state, long-term. PTX is indicated for patients with T1DM and some selected cases of type 2 DM [T2DM], yet it remains underutilized. In fact, in the US, for every 10,000 patients with T1DM, only 3 will actually receive PTX or islet transplant in their lifetime, due to factors such as the lack of suitable pancreas donors, the burden of chronic toxicity determined by lifelong immunosuppression, and other issues related to financing and access to transplantation;[5] when T2DM is considered, only three patients in one million will ever receive PTX or islet transplant. Therefore, the identification of a new, potentially inexhaustible source of β-cells for transplantation is extremely urgent.

Regenerative medicine has shown an immense potential to address the limited number of transplantable organs and to allow immunosuppression-free transplantation.[6–15] Among the different technologies under development, the seeding of cells on supporting scaffolding material (cell-on-scaffold seeding technology, CSST)[16] appears to offer the quickest route to clinical application.[6] This technology is based on the striking evidence that extracellular

matrix (ECM) proteins and structures play fundamental roles in the determination, differentiation, proliferation, survival, polarity, welfare and migration of cells.[17] So far, CSST has allowed the production of numerous, yet relatively simple organs that were eventually implanted in more than 200 patients, for therapeutic purposes.[6] As these body parts were bioengineered from patient's own cells, immunosuppression was never needed. CSST is also being applied to bioengineer more complex organs for transplant purposes. At Wake Forest, we have developed an innovative method that, through the detergent-based decellularization of porcine and human organs, allows successful and consistent production of acellular extracellular matrix (ECM) scaffolds.[18_20]

We envision that when a patient will need beta cell replacement therapy, s/he will be offered a new generation bio-artificial endocrine pancreas (BAEP) consisting of a software and a hardware. The software will be represented by beta cells generated through the *ad hoc* differentiation of either progenitor cells obtained from the patient's pancreas, or induced pluripotent cells reprogrammed from patient's fibroblasts. Patient-derived beta cells will be seeded or embedded in the hardware of the BAEP, namely the 3D framework of ECM scaffolds produced from pancreata of allogenic human origin. To this end, we have tested here our decellularization method to discarded human pancreata and we carefully characterized the molecular, physical, and immune properties of human pancreas acellular ECM scaffolds (hpaECMs) together with their cytocompatibility.

2. Material & Methods

2.1 Pancreas and endothelial cell procurement

Twenty-five human pancreata were processed. Each organ was originally recovered for transplantation, but subsequently discarded as deemed unsuitable for transplantation.

2.2 Pancreas preparation

Organs were received in cold sterile preservation solution after en-bloc removal that included the whole organ pancreas, duodenum and spleen, and then prepared by removing the duodenum and ligating all of the vascular branches from the arterial arcade connecting the pancreatic head with the duodenum. Thereafter, the pancreatic duct (PD) was cannulated with a 14G catheter. The peripancreatic fat was trimmed, the splenic vessels were ligated at the splenic hilum, and the spleen was removed. The superior mesenteric artery (SMA) and proximal stump of the splenic artery (SA) were cannulated using 16G plastic connectors. Pancreata were then washed with 500 ml of saline solution containing 50 ml of betadine and then with 10% Penn/Strep solution. They were eventually rinsed with 500ml of sterile PBS and stored at 4°C.

2.3 Pancreas decellularization

After placing the pancreas in an *ad hoc* container, PD, SMA and SA were connected to a double-line peristaltic pump (Masterflex L/S, easy load pump head and L/S 16G tubing, Cole-Parmer Instrument Co, Vernon Hills, IL, USA) (Fig. 1). Then, the pancreas was flushed with 4°C phosphate buffer solution (PBS) and heparin (1% off 1000 U, 10U/ml) at 6 ml/min for 60 minutes (360 mL total). Afterwards, 1% Triton X-100 and 0,1% ammonium

hydroxide solution was perfused at 12.5 ml/min for 48 hours (72 L total) through both inlets (PD and SMA/SA inlet), at 4°C. The so-obtained hpaECMs was then rinsed with DNAse (D5025–Type IV, deoxyribonuclease from bovine pancreas, Sigma Aldrich, St. Louis, Mo) and 0.0025% magnesium chloride). Finally, scaffolds were perfused with saline at a flow of 6 mL/min for 5 days (12.9000 L total) to remove detergent and stored at 4°C. Scaffolds destined for cell seeding experiments (see below) were sterilized by γ-irradiation (12.000 Gy) and stored in PBS at 4°C. Scaffolds destined for immunological studies were γ-irradiated, lyophilized, and stored at 4°C.

2.4 Bioscaffold characterization

2.4.1 Vessel patency—To evaluate the patency of the hpaECMs' innate vasculature, angiography was performed by injecting 5 ml of contrast agent in each inlet (PD, MSA and SA, 15 mL total) at the flow rate of 25 mL/min.

2.4.2 Collagen and DNA quantification—Collagen and DNA content of fresh and decellularized pancreas was measured through indirect quantification of hydroxyproline residues using the Quick-Zyme Total Collagen Assay (QuicZyme, Biosciences), and using a tissue DNA isolation kit (PureLink Genomic DNA MiniKit, Invitrogen), respectively, as previously described.[20]

2.4.3 Basic histology, immunofluorescence and cellularity—hpaECMs samples were fixed for 24 hours in formalin, washed in diH2O, dehydrated in graded alcohol, embedded in paraffin, 5 mm-sectioned, and eventually stained with H&E, Masson's Trichrome (MT), elastic Van Gieson (EVG), Alcian Blue (AB) and Picrosirius Red (PR). Slides were compared with counterparts obtained from discarded pancreata that did not undergo decellularization.

For immunofluorescence analysis, slides were incubated overnight with primary antibodies against collagen type I (dilution 1:25, Southern Biotech), collagen type IV (dilution 1:100, Southern Biotech), fibronectin (dilution 1:100, Santa Cruz), laminin (dilution 1:200, Sigma), HLA Class I (dilution 1:100, Abcam) and HLA DP+DR+DQ (dilution 1:25, Abcam). Nuclei were counterstained with DAPI. Slides were visualized using fluorescence microscopy (Carl Zeiss) and compared to counterparts obtained from discarded pancreas that did not undergo decellularization.

To quantify the remaining cells after decellularization, a portion of fresh and acellular tissue was frozen in liquid nitrogen and 10 slides of each tissue were analyzed with an optical microscope. The samples were covered with Vectashield (Vector Laboratories, Inc, Burlingame, CA) mounting medium for fluorescence with 40-6-diamidino-2-phenylindole (DAPI) (Vector Laboratories, Inc), and the total number of nuclei per field was counted in random pictures using fluorescence microscopy (Carl Zeiss).

2.4.4 Scanning electron microscopy (SEM)—To evaluate scaffolds' ultrastructure, samples of hpaECMs and normal pancreas were processed and analyzed as previously described.[20] Images were recorded with a Jeol7401 FEG scanning electron microscope.

2.4.5 Chicken chorioallantoic membrane (CAM) angiogenic assay—To assess the angiogenic properties of our scaffolds, we used the CAM assay as previously described.[20_22] Primary endpoint was the number of blood vessels converging towards decellularized matrices, which were counted manually. Only blood vessels less than 10mm in diameter were counted by blinded assessors (n=4), with the mean of the counts being considered.

2.4.6 Measurement of pancreatic tissue stiffness—To assess hpaECMs stiffness, dog bone shaped samples, 4mm wide at the narrowest point with a length of 18mm, were punched from wet pancreas before and after the decellularization process. The mechanical properties were measured using tensile extension by a uniaxial load test machine (Instron5544, Instron Corporation, Issaquah, WA) with an extension rate of 10.0 mm/min. Scaffold's stress-stain curves were recorded and Young's modulus and tensile strength and strain at break were obtained. Six samples were measured for each scaffold allowing the mean and standard deviation to be calculated.

2.4.7 Growth factor (GF) analysis—We hypothesized that GFs, cytokines and chemokines are only partially depleted from our matrices. To validate our hypothesis, we produced 5 hpaECMs from 5 different organs (study group). Two samples were procured from each scaffold (10 pieces total) with a 12mm biopsy punch; the control group consisted of 10 samples obtained in the same fashion from 5 discarded pancreata that did not undergo decellularization. All samples were stored in sterile PBS with 2% pen/strep and then shipped to the manufacturer (Raybiotech, http://www.raybiotech.com), where they were processed using the Quantibody® Human Growth Factor Array Q1.

2.4.8 Immunological studies

a] Isolation of T cells: Peripheral blood mononuclear cells (PBMC) were isolated by Ficoll gradient centrifugation of de-identified buffy coats from healthy donors purchased from the NY blood bank. Naïve $CD4^+$ T cells were enriched over the auto MACS cell separator by negative selection with naïve CD4 T cell isolation kit (Miltenyi Biotec, Inc., Auburn, CA). After isolation, cells were stained for CD4 and CD45RA to confirm purity that was consistently higher than 95%.

b] *In vitro* cultures: carboxyfluorescein diacetate succinimidyl ester (CFSE)-labeled T cells were activated with anti-CD3/anti-CD28 coated Dynabeads (Life Technologies, Grand Island, NY) with or without IL-2 (100U/mL; BD Biosciences, San Jose, CA) and cultured alone or in the presence of lyophilized hpaECMs. Before use, hpaECMs was incubated at 37°C overnight and filtered through a 40 μm strainer. Naïve $CD4^+$ T cells were cultured at 37 in 5% CO_2 atmosphere in complete RPMI plus 10% heat–inactivated human AB serum (regulatory T cell induction experiments were performed with 2% AB serum) for 5 days and then analyzed for CFSE dilution by FACS. CFSE was obtained from Invitrogen (Carlsbad, CA).

c] Antibodies, staining protocols, flow cytometry: Cell surface staining was performed using antibodies against CD4, CD8, and CD25 from eBioscience (San Diego, CA). Appropriate isotype matched monoclonal antibodies were used as controls. To evaluate cell

apoptosis and death, cells were stained with antibodies against Annexin V and 7-AAD (BD Biosciences) in appropriate staining buffer (BD Biosciences). To measure the percentage of $CD4^+CD25^+FoxP3^+$ cells, cells were permeabilized and stained with anti-FoxP3 antibody (eBioscience) according to manufacturer's instructions. Flow cytometric analysis was performed on a FACSCanto II flow cytometer using DiVA software package (BD, Franklin Lakes, NJ). Data were analyzed using CytoBank software (https://www.cytobank.org).

2.5 Assessment of the ability of hpaECMs to sustain cell attachment and growth

a] Human islets—Pancreases were processed using standard Liberase HI collagenase digestion with mechanical dissociation within a Ricordi chamber. Islets were purified with an optiprep discontinuous gradient method, identified and counted using dithizone staining. paECMs samples were prepared as shown in Figure 1, sterilized via γ-irradiation and placed in RPMI with 10% FBS overnight at 4°C, prior to seeding. The day after, 200 islets per scaffold were statically seeded on matrices with fresh media and cultured under standard conditions in RPMI media with 10% FBS for 4 days prior to perifusion testing.[18] As control, additional islets were cultured on standard Petri dishes under the same culture conditions. Briefly, each group of 200 islets was placed into perifusion chambers, either seeded on scaffolds or free. The chambers were then perifused with Krebs-Ringer-bicarbonate (KRB) solution containing 0.2% bovine serum albumin (BSA) at a flow rate of 0.3 mL/min. During the procedure the KRB was continuously gassed with 95% air/5% CO_2. The islets were pre-perifused for 1 hour in a low glucose (3.3 mM) KRB solution prior to sampling. After one hour, effluent samples were collected from the low-glucose KRB solution every 5 minutes for 20 minutes. Then a high-glucose solution (16.7 mM) was perifused through the chambers for 30 minutes with effluent sample collection every 2 minutes. Following the 30 minutes of high glucose, the chambers were perifused again with low-glucose KRB for 30 minutes with samples collection every 5 minutes. The effluent samples were stored at −20°C until analyzed for insulin content via radioimmunoassay. Insulin values are normalized to basal averages, n=4, error bars represent SEM.

b] Human endothelial cells—Human primary pancreatic endothelial cells (hPPECs) were isolated from discarded pancreata as described by Navone et al.[23] Cells were then expanded on matrigel–coated flasks and grew with endothelial proliferation medium (EndoPM). At the time of seeding, 20×10^6 cells were injected with a syringe pump in a whole acellular pancreas scaffold through the SMA and SA, at a flow of 0.2ml/min. Cells were allowed to attach for 2 hours, after which perfusion culture started. Seeded matrices were cultured in a custom-built bioreactor (Fig. 8B). Media were infused through Luer lock access ports and allowed to equilibrate with 5%CO_2 and 95% room air by insertion of 0.22μm filters and magnetic stirring. The system (and the related technical support) was designed and developed by SKE Advanced Therapies.

After 6 days, matrices were fixed in formalin, sampled into 5-μm sections, and stained for H&E, CD31 (clone JC70A, 1:100, DAKO), Ki67 (clone Mib1, 1:600, DAKO) using standard protocols. Antigen retrieval was performed with Tris EDTA pH 9 for both antibodies. The percentage of Ki67+ cells was obtained as the ratio of Ki67+ and

hematoxylin+ cells. Immunohistochemistry and H&E-stained images were recorded using Aperio Scan System (Leica Microsystems).

3. Results

3.1 Human pancreas decellularization

Triton-based perfusion allowed complete clearance of the cellular compartment of discarded pancreata (Fig. 1A–B). Fluoroscopy depicted an intact vascular network that retained the hierarchical branching structures (Supplementary Fig. 1C–G). In fact, contrast media flowed progressively from larger vessels to smaller capillaries to eventually drain out through the venous outlets, without extravasating within the hpaECMs.

3.2 Collagen and DNA quantification

To investigate the ability of the decellularization protocol to maintain ECM components of the native pancreas, fresh and acellular samples were processed for collagen quantification. Quantitative assay showed statistically increased collagen in acellular matrices compared to fresh tissue (from 22.9±10.0 to 75.4±16.8 μg/mg, $P<0.001$).

DNA analysis was performed as indirect proof of successful decellularization and demonstrated approximately 99% clearance of DNA in comparison with the native organ (from 1.35±0.43 to 0.04±0.03 μg/mg, $P<0.001$) (Fig. 1H).

3.3 Basic histology, immunofluorescence and cellularity

Fresh and acellular samples were processed for Masson trichrome, Picrosirius red, elastic Van Gieson and Alcian blue (Fig. 2). All stainings confirmed complete absence of nuclear material and cells, consistent with the H&E and DAPI findings. Masson trichrome and Picrosirius red revealed preservation of collagen fibers. Alcian blue staining indicated preservation of sulfated glycosaminoglycan proteins. Elastic Van Gieson staining showed that elastin was retained after decellularization.

DAPI and H&E staining, as well as immunofluorescence for both HLA class I and class II antigens confirmed the complete clearance of the cellular compartment of the hpaECMs (Fig. 3A). The scaffolding architecture of the pancreas was well preserved. In fact, H&E staining showed the pink eosinophilic staining typical of collagen in the absence of any basophilic staining indicative of cellular nuclear material (Fig. 2). Specific nuclei staining with DAPI confirmed the absence of cell nuclei after decellularization; this finding was also supported by the count of the total number of nuclei per field in random pictures (from 410±120 to 0 nuclei, $P<0.001$). As an indirect sign of successful decellularization, neither HLA class I or class II positive cells were seen in the pancreatic matrices.

Immunofluorescence for specific ECM molecules that have a significant role in the pancreatic parenchyma was performed for a fuller characterization of our scaffolds. Immunostaining detected the presence of laminin, collagen I, collagen IV and fibronectin in the native pancreas (Fig. 3B). Laminin detection in the acellular matrix showed strong positivity similar to fresh tissue, especially around vessels and structures resembling the native sites of the islets. In contrast, preservation of collagen I (Fig. 3B) was less evident

with respect to the fresh pancreatic ECM, while immunofluorescence for collagen IV and fibronectin Fig. 3C) showed specific distribution of both components at the same level of native tissue.

3.4 Scanning Electron Microscopy (SEM) analysis

SEM revealed retained nanofibrous structures in hpaECMs and confirmed absence of intact cells, suggesting that the decellularization process produced an acellular matrix scaffold that retained the micro- and ultra-structural details of pancreas architecture (Fig. 4).

3.5 CAM assay

To test the ability of hpaECMs to induce neo-angiogenesis, samples of matrix were implanted *in ovo*. CAM assay showed that the scaffolds integrated well with the developing environment of the chicken egg and representative images of the implanted scaffolds at 0 and 7 days of incubation demonstrated generation of capillaries around and above the scaffolds (Supplemtary Figure 1, top). Neoangiogenesis was quantified by manually counting the total number of blood vessels converging towards matrices. Seven days after implantation, the number of vessels growing towards the acellular scaffolds was significantly increased in comparison to the same sample at day 0 ($P<0.05$) and to the filter membrane loaded with PBS that was used as a negative control ($P<0.05$) (Supplementary Fig. 1, bottom). Interestingly, the pro-angiogenic effect of hpaECMs was comparable with VEGF-loaded membrane used as positive control ($P>0.05$).

3.6 Acellular scaffold stiffness properties

It has been proposed that the ECM has the ability to maintain the original mechanical properties of native organs. By assessing the mechanical properties of our scaffolds, we were able to partially elucidate the influence of the decellularization process on ECM in terms of destruction, degradation and/or decomposition. The properties of native pancreas were compared with that of hpaECMs. The results showed that the Young's modules and tensile strain at break had slight decreases, but no significant difference after the removal of cellular components, changing from 0.165±0.039 MPa and 96.71±39.67% to 0.139±0.052 MPa and 76.22±22.23% respectively (Supplementary Fig. 2). The tensile stress at break of decellularized pancreata (0.070±0.017MPa) was comparable to the native pancreas (0.068±0.006MPa) ($P<0.05$). These results indicated that the ECM plays a prominent role in determining the mechanical properties of the pancreas, and that our decellularization method effectively maintains the integrity of the tissue's ECM without destruction or degradation.

3.7 hpaECMs retain GFs

Data obtained from the quantitative array platform showed that several GFs were still present in the hpaECMs after decellularization. Some of these molecules are essential in angiogenesis and vasculogenesis, cell development, neuronal growth and regeneration, as well as insulin level and glucose homeostasis (Supplementary Table 1). Intriguingly, hpaECMs also contains TGF-β1, a cytokine with immune modulating effects [4].

3.8 hpaECMs immune effects

a] hpaECMs inhibits naïve CD4+ T cell expansion—To test effects of hpaECMs on human naïve $CD4^+$ T-cell function, we stimulated CFSE-labeled naïve $CD4^+$ T cells with anti-CD3/anti-CD28 mAbs in the presence or absence of hpaECMs and quantified proliferation by CFSE dilution using flow cytometry. These assays showed a statistically significant inhibitory effect of hpaECMs on naïve $CD4^+$ T cell proliferation (Fig. 5A–B).

b] hpaECMs induces T cell apoptosis—To investigate whether hpaECMs inhibitory effects on T cell proliferation was associated with T cell apoptosis, we activated T cells with anti-CD3/anti-CD28 and we cultured them with or without hpaECMs. On day 5 of culture, we stained cells for Annexin V and 7-AAD and found a significant increase in cell apoptosis/necrosis when cells were cultured in the presence of hapECMs (Fig. 5C–D).

c] hpaECMs induces conversion of naïve CD4+ T cells into regulatory T cells (Treg)—Through their capacity of inhibiting effector T cell expansion and function, Treg are essential for immune homeostasis and are critical for tolerance induction and maintenance in organ transplantation.[24] There are two major subsets of $CD4^+$ Treg: thymus-derived $CD4^+CD25^+Foxp3^+$ Treg and inducible Treg that develop from naïve T cells in the periphery under tolerogenic conditions.

Since TGF-β is crucial for Treg induction and ECM contains TGF-β, we hypothesized that ECM promoted conversion of naïve $CD4^+$ T cells into Treg. To test this hypothesis, we performed *in vitro* Treg induction assays by stimulating naïve $CD4^+$ T cells with anti-CD3/anti-CD28 mAbs, IL-2, with or without hpaECMs. The presence of hpaECMs significantly increased the percentage of $CD4^+CD25^+FoxP3^+$ Treg at the end of the culture (Fig. 5E–F).

3.9 Cell Seeding of acellular pancreatic scaffold

a] Human Islets—Islets stained positive for DTZ on both scaffolding (Fig. 6D) and culture dishes (Fig. 6C). Both islets seeded on scaffolds and islets on culture dishes were functional following 4 days of culture with similar stimulation indices (as defined as the peak insulin secretion rate divided by the basal insulin secretion rate) of 2.81±0.48 and 3.44±1.821 respectively ($p=0.59$, average ± standard deviation, $n=3$) (Fig. 6E). These data clearly demonstrate that the decellularized scaffold did not cause any toxicity to the islet cells seeded on it.

b] Human endothelial cells—hapECM was seeded with human pancreatic endothelial cells. Pancreatic tail was surgically isolated in order to obtain a smaller volume to seed, keeping at the same time an inflow and an outflow (Fig. 7A). Matrix was seeded with cells and cultured for six days in a bioreactor, consisting in a closed circuit with one chamber for organ housing, a reservoir for medium oxygenation and a peristaltic pump (Fig. 7B). At H&E, cells were ubiquitous within the matrices, yet tended to localize at the level of small and large vessels. Cells distributed in a line on the edges of the vessel walls resembling primitive structures of vessel formation (Fig. 7C). All cells confirmed their endothelial nature as evidenced by CD31 staining. More than 50% of cells were proliferating, as

determined by Ki67 staining, demonstrating that a mid-term culture in the acellular scaffold allows cell survival and proliferation (Fig. 7D).

4. Discussion

This study represents a progression from previous work that we performed in the porcine pancreas, which supported our hypothesis that ECM scaffolds generated from native pancreas tissue can serve as a platform for insulin-producing bioengineered tissue.[4,18,25] The importance of transitioning to human organs is obvious in the context of clinical relevance. Our results indicate that whole discarded human pancreata can be consistently and successfully decellularized through detergent-based perfusion methodology. Indeed, clearance of cells and HLA class I and II antigens is achieved despite preservation of the ECM's architecture, composition and mechanical properties. In addition, the framework of the vascular network remains intact at all hierarchical levels. Interestingly, for the first time we report that numerous GFs are retained in significant amounts within the 3D structure of our hpaECMs. Some of these GFs are key players in essential pathways such as angiogenesis, cell proliferation and glucose metabolism, and their presence may justify the scaffold's ability to induce angiogenesis in the CAM assay. Importantly, we documented that hpaECMs inhibits naïve $CD4^+$ T cell proliferation, promotes their apoptosis, and induces their conversion into Tregs.[26]

Our data obtained with discarded human pancreas are consistent with our previous experience with discarded human kidneys.[20] However, in contrast to that experience, we used Triton rather than the more aggressive SDS for two reasons: first, because the pancreas texture is less dense then the kidney's, which is basically refractory to nonionic detergents such as Triton; second, we believe that pancreatic enzymes released during cell breakdown occurring during the decellularization process can, in turn, contribute to further clearance of the cellular compartment. Moreover, our study builds on our preliminary experiments with the porcine pancreas,[18] in which we subjected the organs to a 24-hour cycle of decellularization with Triton-based solution. Nevertheless, in the case of discarded pancreata, we used a 48-hour decellularization cycle – twice the length – that was infused through three different inlets (PD, SMA and SA), rather than just two, namely the PD and the superior mesenteric vein. We did so following initial unsuccessful attempts while using only the original two inlets, 24-hour approach, in which we observed a frank impairment of the decellularization process possibly attributable to the significant tissue damage that had justified discard. Overall, we hypothesized that the 3-inlet approach – namely, PD, SMA and SA – would be crucial to successful decellularization, as it would allow ad hoc delivery of the detergent throughout the whole pancreas; and that the higher volume would possibly circumvent hurdles deriving from organ damage such as steatosis and fibrosis.

Previous studies reported immunomodulatory properties of the innate ECM in rodents.[27_30] Our studies for the first time document the immunosuppressive, Treg-promoting properties of our hpaECMs. Though further studies are needed to understand the mechanisms of the immune properties of our matrices, these effects can be – at least in part – attributed to the presence of TGF-β within the matrix that may induce T cell apoptosis and promote conversion of naïve $CD4^+$ T cells into $CD4^+CD25^+FoP3^+$ Treg.[26] As we did not investigate

whether SDS remains in our acellular scaffolds, we cannot formally rule out the possibility that hpaECMs-induced T cell apoptosis is related to the presence of residues of detergent used for decellularization. However, the effect of our matrix on Treg induction and – more importantly – the evidence that both islets and endothelial cells are well viable and functional when seeded on hpaECMs, make this option unlikely. Altogether, these important data support the use of hpaECMs as a matrix to generate bioengineered pancreases and pave the way to further studies on the therapeutic use of hpaECMs as immunosuppressant.

In order to assess hpaECMs cytocompatibility, we used islets and a unique endothelial cell line isolated from the human pancreas, namely hPPECs. In both cases, findings show that our matrices are both islet- and cell-friendly, as they allow attachment, function and maintain the initial phenotype. In the attempt to assess cytocompatibility, while the choice of islets is obvious, hPPECs are justified because we envision that when this technology is successfully translated into the clinic, the first step to follow the production of hpaECMs will be the reconstitution of the endothelium starting from patient's own endothelial cells. In line with our experience with renal ECM scaffolds produced from discarded kidneys, it is important to emphasize that the strategy of using discarded organs introduces a new type of biomaterial, represented by natural scaffolds obtained from the manipulation of organs with pre-existing damage.

Whether hpaECMs will represent a genuine platform for organ bioengineering investigations, still needs to be confirmed, but early results are encouraging and pave the way for further investigations aiming at understanding the mechanisms of interactions between the matrix and the cells, and at identifying the optimal cell type/s to use in order to achieve complete regeneration of the endothelium and islets.

Supplementary Material

Refer to Web version on PubMed Central for supplementary material.

Acknowledgments

Andrea Peloso received a grant from the Fondazione Banca del Monte di Lombardia – Progetto Professionalità Ivano Becchi. We acknowledge Carolina Donor Services and LifeShare of the Carolinas for their invaluable support. Giuseppe Orlando's research is supported by unrestricted funds from Liberitutti Foundation (http://www.liberituttionlus.org/ricerca-medicina-rigenerativa.html).

Abbreviations

DM	diabetes mellitus
ECM	extracellular matrix
OBR	organ bioengineering and regeneration
SEM	scanning electronic microscopy
DAPI	4,6-diamidino-2-phenylindole
IHC	immunohistochemistry

hpaECMs	human pancreas acellular ECM scaffolds
BAEP	bio-artificial endocrine pancreas
hPPECs	human primary pancreatic endothelial cells

References

1. http://www.cdc.gov/diabetes/pubs/estimates11.htm
2. Boyle JP, Thompson TJ, Gregg EW, et al. Projection of the year 2050 burden of diabetes in the US adult population: dynamic modeling of incidence, mortality, and prediabetes prevalence. Popul Health Metr. 2010; 8:29. [PubMed: 20969750]
3. American Diabetes Association. Economic costs of diabetes in the U.S. in 2012. Diabetes Care. 2013; 36:1033–1046. [PubMed: 23468086]
4. Orlando G, Gianello P, Salvatori M, et al. Cell replacement strategies aiming at reconstitution of the beta cell compartment in type 1 diabetes. Diabetes. 2014; 63:1433–1444. [PubMed: 24757193]
5. Orlando G, Stratta RJ, Light J. Pancreas transplantation for type 2 diabetes mellitus. Curr Op Org Transpl. 2011; 16:110–115.
6. Orlando G, Soker S, Stratta RJ. Organ bioengineering and regeneration as the new Holy Grail of organ transplantation. Ann Surg. 2013; 258:221–232. [PubMed: 23782908]
7. Orlando G, Wood KJ, De Coppi P, et al. Regenerative medicine as applied to general surgery. Ann Surg. 2012; 255:867–880. [PubMed: 22330032]
8. Orlando G. Immunosuppression-free transplantation reconsidered from a regenerative medicine perspective. Exp Rev Clin Immun. 2012; 8:179–187.
9. Orlando G, Wood KJ, Soker S, et al. How regenerative medicine may contribute to the achievement of an immunosuppression-free state. Transplantation. 2011; 92:e36–e38. [PubMed: 21989270]
10. Orlando G. Transplantation as a subfield of regenerative medicine. An interview by Lauren Constable. Expert Rev Clin Immunol. 2011; 7:137–141. [PubMed: 21426251]
11. Orlando G, Wood KJ, Stratta RJ, et al. Regenerative medicine and organ transplantation: Past, present and future. Transplantation. 2011; 91:1310–1317. [PubMed: 21505379]
12. Orlando G, Baptista P, Birchall M, et al. Regenerative medicine as applied to solid organ transplantation: current status and future development. Transpl Int. 2011; 24:223–232. [PubMed: 21062367]
13. Badylak SF, Weiss DJ, Caplan A, et al. Engineered whole organs and complex tissues. Lancet. 2012; 379:943–952. [PubMed: 22405797]
14. Badylak SF, Taylor D, Uygun K. Whole-organ tissue engineering: decellularization and recellularization of three-dimensional matrix scaffolds. Ann Rev Biomed Eng. 2011; 13:27–53. [PubMed: 21417722]
15. Soto-Gutierrez A, Wertheim JA, Ott HC, et al. Perspectives on whole-organ assembly: moving toward transplantation on demand. J Clin Invest. 2012; 122:3817–3823. [PubMed: 23114604]
16. Salvatori M, Peloso A, Katari R, et al. Semi-xenotransplantation: combining transplantation with organ bioengineering and regeneration technologies to manufacture complex modular organs. Xenotransplantation. 2015; 22:1–6. [PubMed: 25041180] Mirmalek-Sani A, Orlando G, McQuilling J, et al. Porcine pancreas extracellular matrix as a platform for endocrine pancreas bioengineering. Biomaterials. 2013; 34:5488–5495. [PubMed: 23583038]
17. Hynes RO. The extracellular matrix: not just pretty fibrils. Science. 2009; 326:1216–1219. [PubMed: 19965464]
18. Mirmalek-Sani A, Orlando G, McQuilling J, Pareta R, Mack D, Salvatori M, Farney AC, Stratta RJ, Atala A, Opara EC, Soker S. Porcine pancreas extracellular matrix as a platform for endocrine pancreas bioengineering. Biomaterials. 2013; 34(22):5488–5495. [PubMed: 23583038]
19. Orlando G, Farney A, Sullivan DC, et al. Production and implantation of renal extracellular matrix scaffolds from porcine kidneys as a platform for renal bioengineering investigations. Ann Surg. 2012; 256:363–370. [PubMed: 22691371]

20. Orlando G, Booth CL, Wang Z, et al. Discarded human kidneys as a source of ECM scaffolds for kidney regeneration technologies. Biomaterials. 2013; 34:5915–5925. [PubMed: 23680364]
21. Baiguera S, Macchiarini P, Ribatti D. Chorioallantoic membrane for in vivo investigation of tissue-engineered construct biocompatibily. J Biomed Mater Res. 2012; 100:1425e34.
22. Totinelli G, Maghsaudlou P, Garriboli M, et al. A rat decellularized small bowel scaffold that preserves villus crypt architecture for intestinal regeneration. Biomaterials. 2012; 33:3401e10. [PubMed: 22305104]
23. Navone SE, Marfia G, Invernici G, et al. Isolation and expansion of human and mouse brain microvascular endothelial cells. Nat Protoc. 2013; 8:1680–1693. [PubMed: 23928501]
24. Burrell BE, Nakayama Y, Xu J, Brinkman CC, et al. Regulatory T cell induction, migration, and function in transplantation. J Immunol. 2012; 189:4705–4711. [PubMed: 23125426]
25. Salvatori M, Peloso A, Zambon JP, et al. Extracellular Matrix Scaffold Technology for Bioartificial Pancreas Engineering: State of the Art and Future Challenges. J Diabetes Sci Technol. 2014; 8:159–169. [PubMed: 24876552]
26. Becker C, Fantini MC, Neurath MF. TGF-beta as a T cell regulator in colitis and colon cancer. Cytokine Growth Factor Rev. 2006; 17:97–106. [PubMed: 16298544]
27. Fishman JM, Lowdell MW, Urbani L, et al. Immunomodulatory effect of a decellularized skeletal muscle scaffold in a discordant xenotransplantation model. Proc Natl Acad Sci. USA. 2013; 110:14360–14365. [PubMed: 23940349]
28. Zang M, Zhang Q, Chang EI, et al. Decellularized tracheal matrix scaffold for tracheal tissue engineering: in vivo host response. Plast Reconstr Surg. 2013; 132:549e–559e.
29. Ma R, Li M, Luo J, et al. Structural integrity, ECM components and immunogenicity of decellularized laryngeal scaffold with preserved cartilage. Biomaterials. 2013; 34:1790–1798. [PubMed: 23228420]
30. Brown BN, Valentin JE, Stewart-Akers AM, et al. Macrophage phenotype and remodeling outcomes in response to biologic scaffolds with and without a cellular component. Biomaterials. 2009; 30:1482–1491. [PubMed: 19121538]

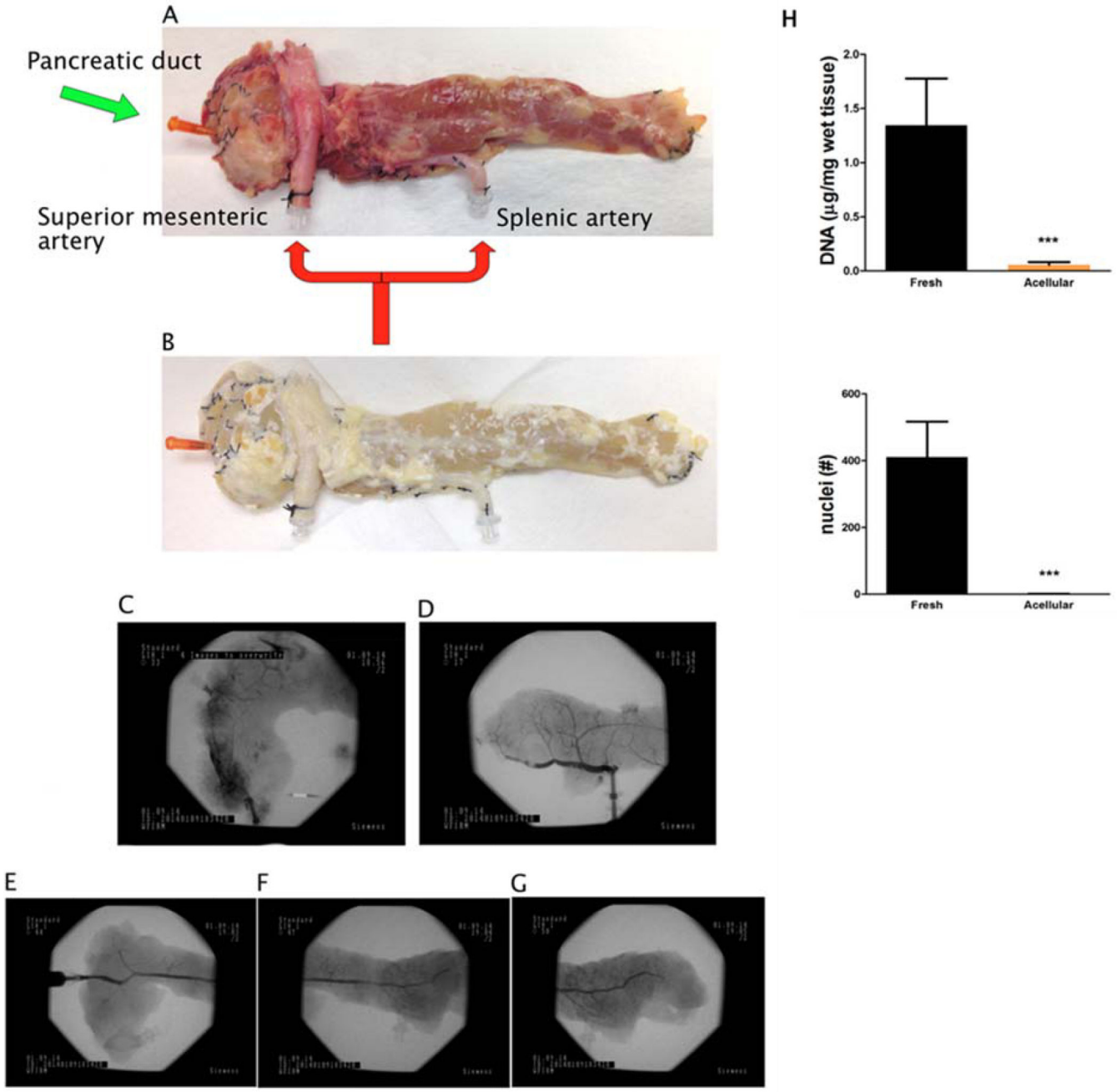

Figure 1.

Decellularization process, fluoroscopy and DNA quantitation. Panels A and B show the set-up of the core for organ decellularization in a discarded human pancreas before and after the treatment. Red arrows in the first image show the arterial, represented by superior mesenteric artery (SMA) and splenic artery (SA) that share one of the two detergent inflows. Green arrow indicates the second inflow through the pancreatic duct (PD). Notably, during decellularization, the color of the organ macroscopically changed from a golden brown color to straw yellow but without reaching the whitish color described for porcine pancreas scaffolds [20]. Fluoroscopy of hpaECMs performed through SMA (Panel C), SA (panel D)

and PD (panel E, F, G). Contrast media flows within the framework of the innate vasculature of hpaECMs without extravasation. Panel H confirms satisfactory cell and DNA clearance. Statistic was made by t-test of fresh vs. acellular tissue; *** $p<0.001$.

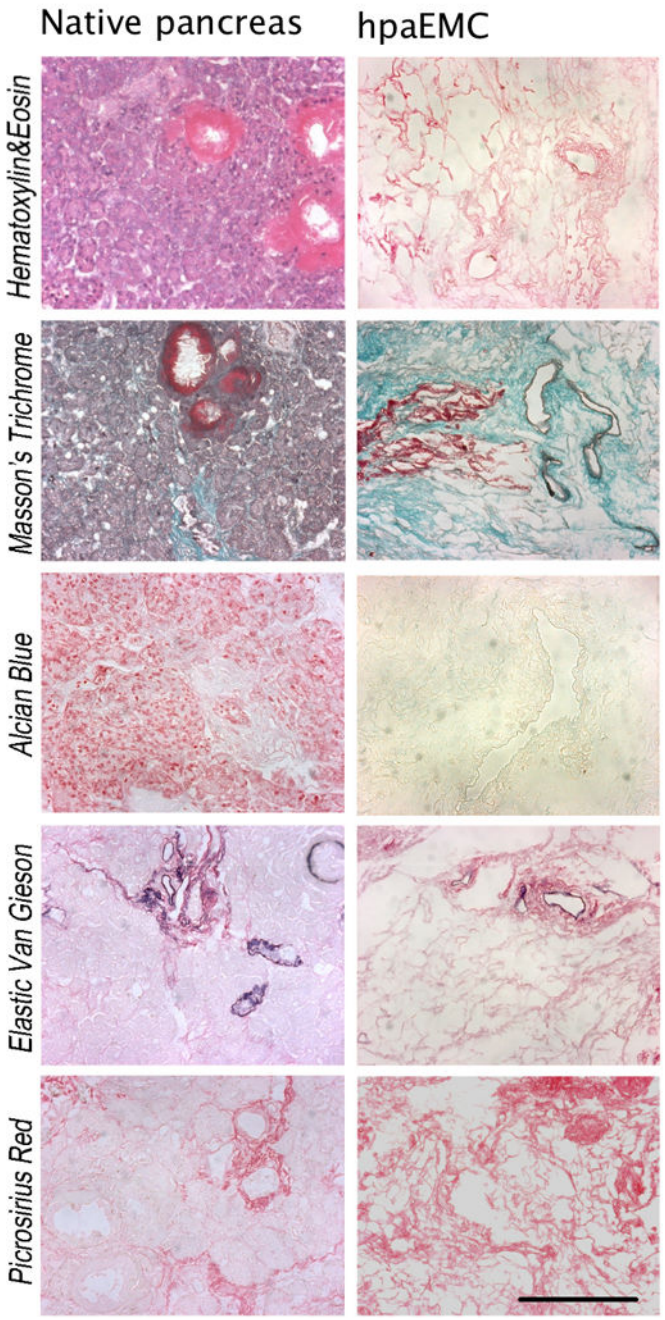

Figure 2.

Basic histology of hpaECMs as compared to the native pancreas. H&E demonstrates complete loss of cellular elements with preservation the intercellular framework. The larger empty spaces on the left aspect of the section almost certainly reflect pathological lesions the nature of which cannot be ascertained with confidence without having examined the sections before treatment, although one can speculate that they represent focal fat necrosis. Masson trichrome shows the light green ECM framework. On the left aspect of the right panel there is evidence of scarring indicated by the dense area staining green.

Alcian blue demonstrates preservation of the so-called ground substance in the connective tissue framework, although the process of digestion involved in decellularization has altered the faint blue color of Alcian blue into a faint green color as can be seen in the right panel.
The van Gieson stain demonstrates preservation of elastine.
The picrosirius red demonstrates abundant collagen in the right panel, reflecting significant scarring in the field photographed in contrast to the left panel.

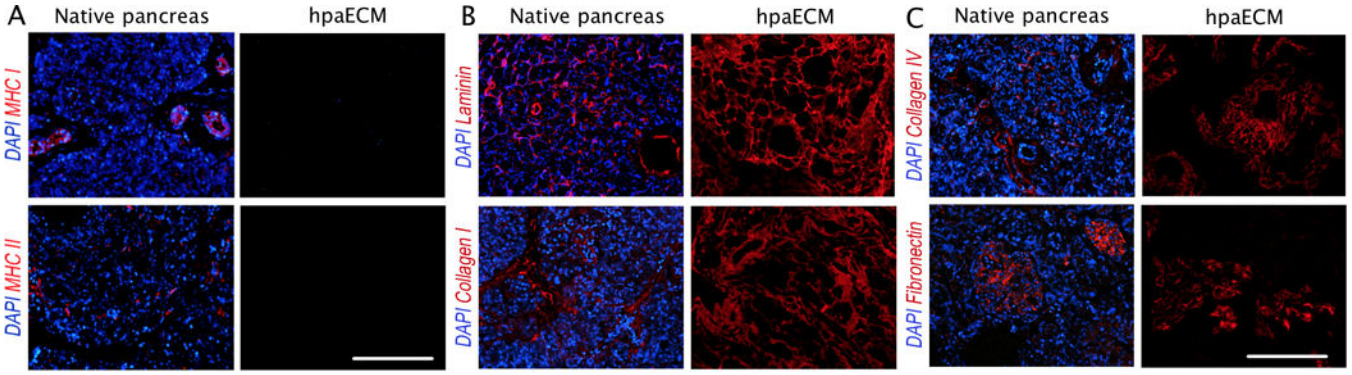

Figure 3.

Immunohistochemistry. Aside of nuclear staining, presence of possible immunogens was ruled out by immunostaining for major histocompatibility complex of class I and II (HLA I and II). Immunostaining for critical, ubiquitous components of pancreas ECM showed that laminin, fibronectin, collagen type I and IV remains well preserved in hpaECMs (nuclei were conterstained with DAPI) and displays a similar distribution of these proteins in the fresh and decellularized pancreas bioscaffold sections.

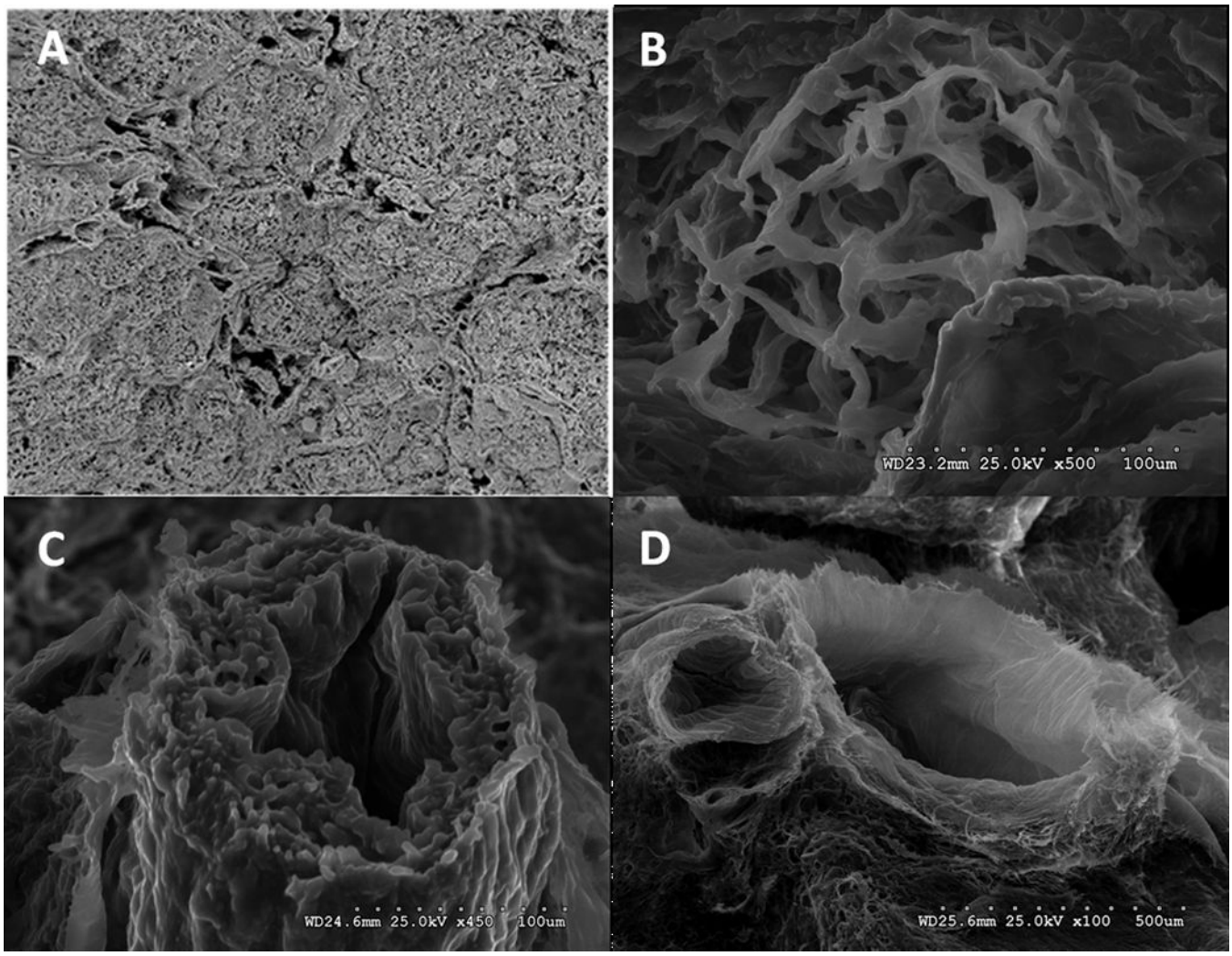

Figure 4.

SEM of intact and acellular pancreas ECM. A. Low power magnification of a cross section through the decellularized pancreas demonstrating preservation of the ECM supporting the exocrine and endocrine elements as well as the vasculature. B. Three dimensional view of the ECM framework of an islet of Langerhans in the decellularized pancreas, identifiable by what is presumably its spherical microvascular framework. C. Cross-section through what we interpret as an arteriole with the lumen delimited by the internal elastic membrane and external to it the individual layers of basement membrane of dissolved smooth muscle fibers of the arteriole's media. D. A presumed venule identifiable by the smaller number of layers of smooth muscle cells (identified by the layers of basement membrane) forming its wall and two small tributaries presumed to be contributing to its formation.

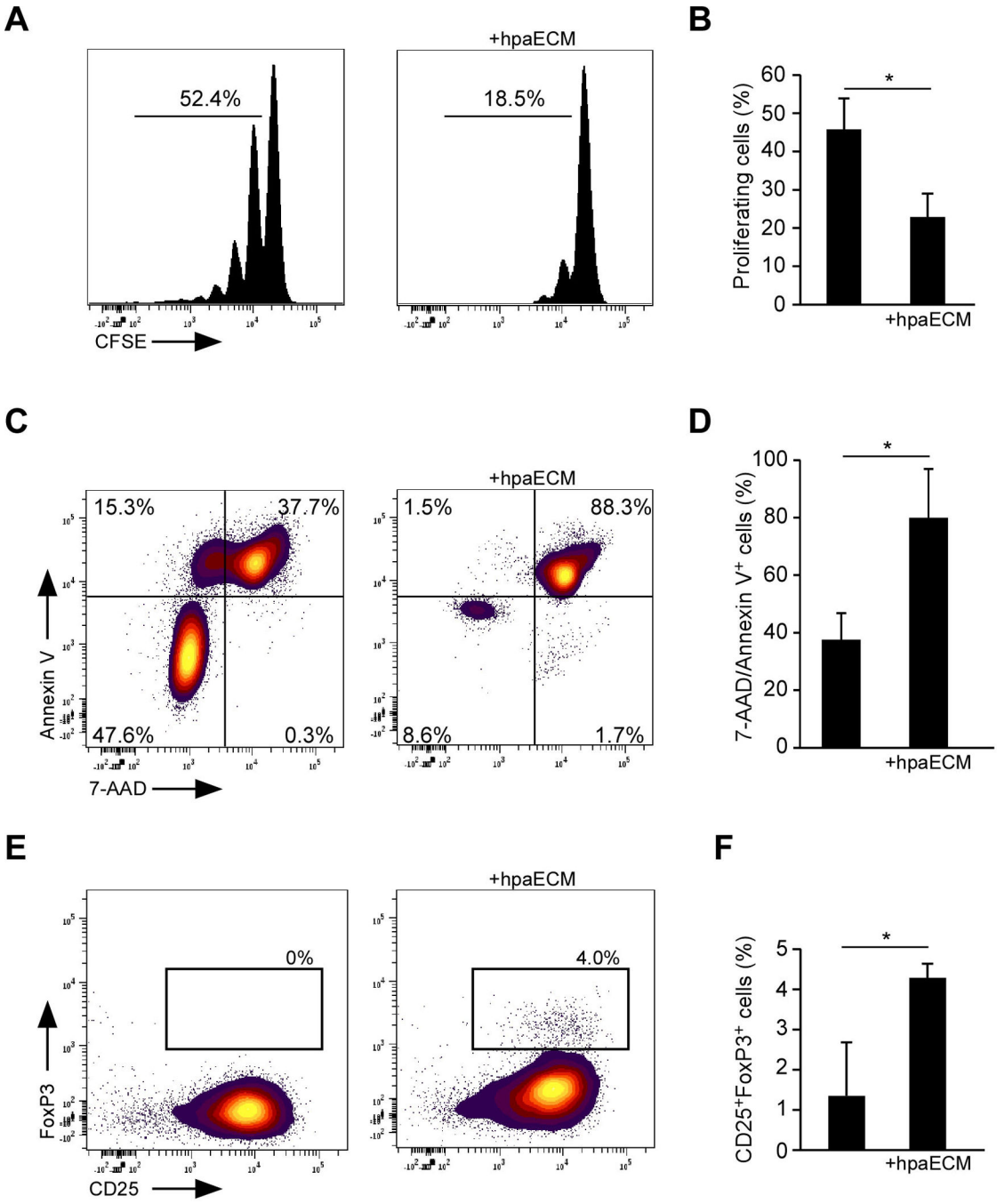

Figure 5.

Immune properties of hpaECM. (A) Representative plots and (B) quantitation of CFSE dilution in CFSE-labeled human naïve $CD4^+$ T cells stimulated with anti-CD3/anti-CD28 coated beads cultured with or without hpaECM. (C) Representative plots and (D) quantitation of Annexin-V and 7-AAD expression as a measure of apoptosis/necrosis in human naïve $CD4^+$ T cells stimulated with anti-CD3/anti-CD28 coated beads cultured with or without hpaECM. (E) Representative plots and (F) quantitation of FoxP3 expression in $CD4^+CD25^+$ cells converted from human naïve $CD4^+$ T cells stimulated with anti-CD3/anti-

CD28 coated beads and IL2 cultured with or without hpaECM. All experiments were analyzed on day 5. Data are means+SD; four experiments). *P<0.05.

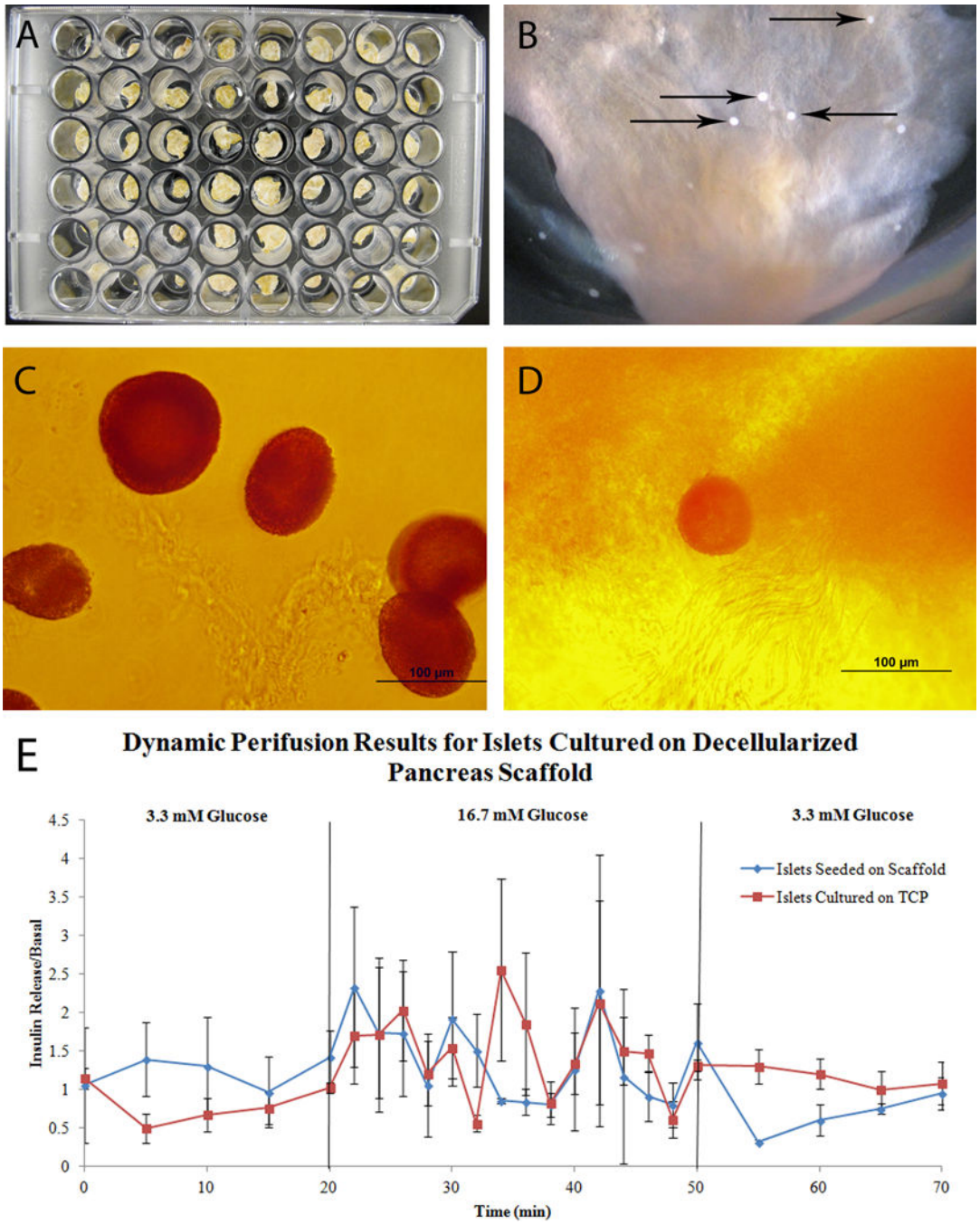

Figure 6.

Evaluation of islets seeded onto decellularized scaffolds. (A) Decellularized scaffolds prior to seeding. (B) Scaffold immediately after seeding, black arrows indicate islets. (C) Dithizone stained islets after 4 days in culture on culture plates. (D) Dithizone stained islet located on periphery of scaffold, 4 days after seeding onto scaffolds. (E) Glucose stimulation index (GSI) for human islets after 4 days in culture. In order to determine the functionality of islets following 4 days of culture dynamic perifusion tests were conducted. 200 islets were placed into perifusion chambers, either seeded on scaffolds or free. The chambers were

then perfiused with Krebs-Ringer-bicarbonate (KRB) solution containing 0.2% bovine serum albumin (BSA) and either 3.3 mM or 16.7 mM glucose at a flow rate of 0.3 mL/min with continuous gassing with 95% air/5% CO2 and effluent sample collection. The effluent samples were stored at −20°C until analyzed for insulin content by radioimmunoassay. The glucose stimulation index defined as the ratio of insulin secreted during the high glucose period normalized to the insulin secreted during the basal glucose period was then calculated. Both islets in standard culture conditions as well as islets seeded on scaffold demonstrated similar responses to changes in glucose concentration. Data represent mean + standard deviation, n=3. TCP denotes tissue culture plate.

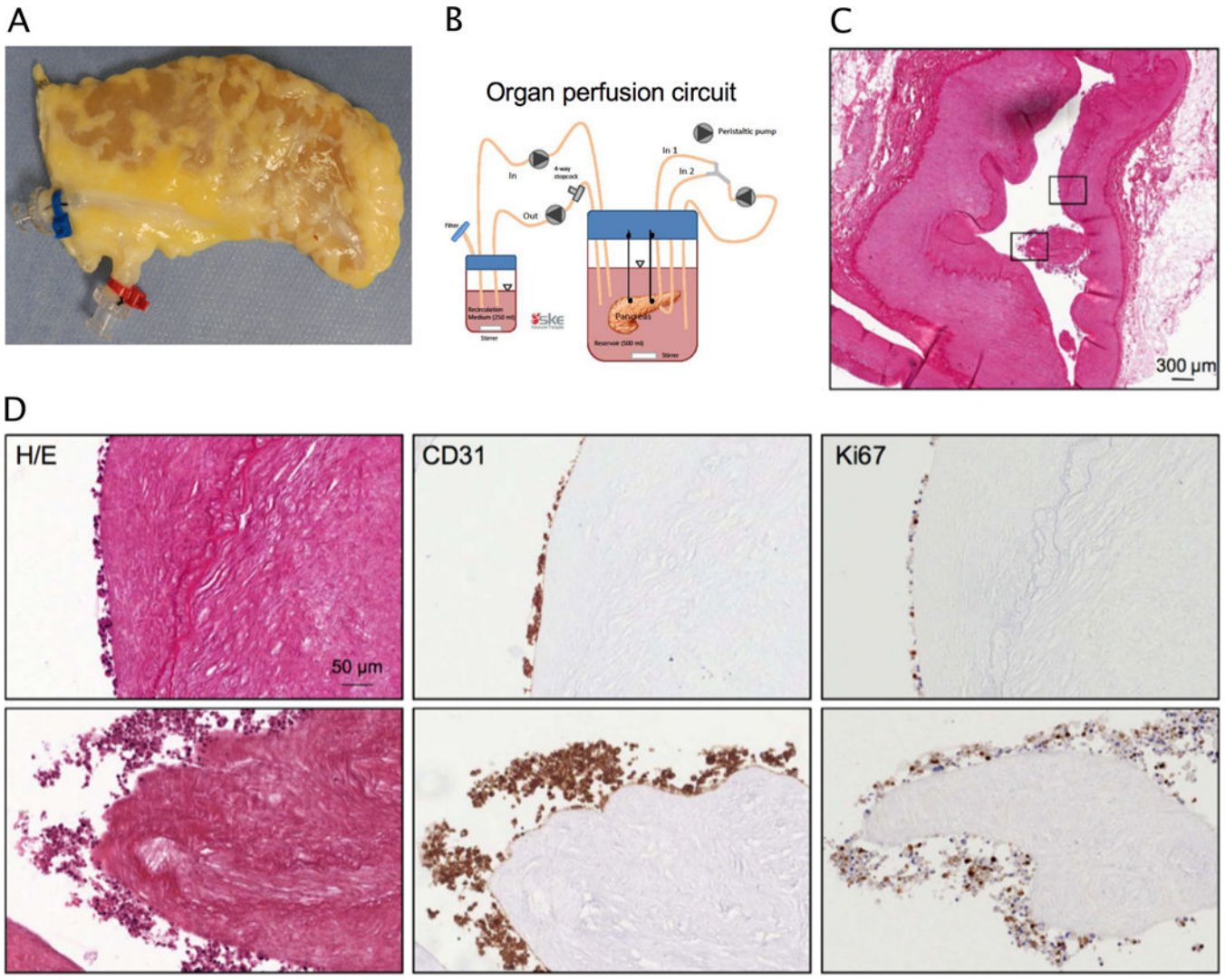

Figure 7.

Endothelial cell seeding. Matrix was seeded with human pancreatic endothelial cells and cultured for six days in a bioreactor, consisting in a closed circuit with one chamber for organ housing, a reservoir for medium oxygenation and a peristaltic pump (Ismatec), connected by tubing (ID 1/16", Pharmed BPT) Pancreatic tail was surgically isolated in order to obtain a smaller volume to seed keeping at the same time an inflow (SA – red connector) and an outflow (Splenic Vein -SV- blue connector) (Panel A). Panel B indicates a schematic representation of the perfusion circuit for seeded pancreatic scaffold culture. Panel C shows a representative image of H&E stain showing localization of infused cells in vessels. Boxes indicate areas reported with high magnification in the panel below. Panel D illustrates representative images of H&E (left), CD31 (middle) and Ki67 (right) matrix staining.